Energy & Buildings 343 (2025) 115907

Contents lists available at ScienceDirect

Energy & Buildings

journal homepage: www.elsevier.com/locate/enb

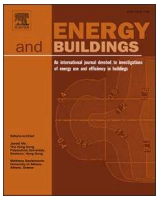

A novel energy system designed to cover electricity, heat, hydrogen and propane for decarbonized buildings☆

Moslem Sharifishourabi *, Ibrahim Dincer, Atef Mohany

Clean Energy Research Laboratory, Faculty of Engineering and Applied Science, Ontario Tech. University, 2000 Simcoe Street North, Oshawa, Ontario L1G 0C5, Canada

ARTICLE INFO

Keywords:
Solar energy
Energy efficiency
Sustainable community
Biomass pyrolysis
Clean propane production
Multigeneration energy system
Hydrogen production
Exergy

ABSTRACT

This study presents an innovative approach to develop an integrated solar-biomass energy system which is essentially designed to simultaneously generate electricity, heat, hydrogen, and propane by addressing all of the possible energy demands of buildings. The system uses solar energy through a steam Rankine cycle and utilizes biomass pyrolysis to maximize efficiency and sustainability, with biochar as a valuable byproduct. The specific thermodynamic analysis reveals the energy and exergy efficiencies of 65.7 % and 64.6 %, respectively. The system schieves high production capacities by generating 1,688 kW of net electricity, 9,518 kW of heat, 49.02 kg/h of hydrogen, and 1,094.29 kg/h of propane. Some parametric analyses highlight the impact of key variables, such as thermal storage temperature, pyrolysis pressure, and steam flow rate, on system performance. Increasing the thermal storage temperature from 600 °C to 700 °C improves both energy and exergy efficiencies while improving heat and propane output. Additionally, pyrolysis conditions significantly influence hydrogen and propane yields, with hydrogen production peaking at 53.28 kg/h at 1.5 bar. This innovative design provides a pathway to efficient, low-carbon energy generation, underscoring the potential of integrated renewable systems to meet the building sector's energy demands and sustainability goals.

1. Introduction

As the global population grows, the demand for energy rises proportionally to accommodate the growing needs of households, industries, and services. This heightened demand significantly affects electricity consumption, which supports several applications, including heating, cooling, industrial machinery, and everyday household appliances [1]. A substantial share of this energy is used for heating water across residential, commercial, and industrial sectors, a process traditionally reliant on fossil fuels [2]. It's important to note that current methods of propane production, a common source for heating, are not environmentally friendly either [3]. Traditional methods of propane production primarily involve its separation as a byproduct during natural gas processing and crude oil refining. In natural gas processing, raw gas is treated to remove impurities and separate hydrocarbons, namely propane, butane and ethane. Similarly, during crude oil refining, propane is extracted in the fractional distillation process, typically from the lighter fractions of petroleum. These methods rely heavily on fossil fuel reserves and are integral to the production of liquefied petroleum gas (LPG), of which propane is a significant component [4]. To mitigate the environmental impact of fossil fuel-based heating, there is a growing emphasis on decarbonized buildings [5]. These structures utilize energy-efficient designs and integrate renewable energy sources such as solar and geothermal to reduce reliance on traditional heating fuels. Decarbonized buildings do not only lower greenhouse gas emissions but also improve energy efficiency, making them a crucial component of the global transition toward sustainable energy solutions. For instance, solar energy, harnessed through photovoltaic (PV) panels and concentrated solar power (CSP) systems, offers a clean and sustainable alternative for electricity generation [6]. The Earth receives approximately 174 petawatts of incoming solar radiation at the upper atmosphere, with about 122 petawatts absorbed by clouds, oceans, and land masses. This abundant energy resource is available worldwide, making it a viable option to reduce fossil fuel dependency and significantly cut carbon emissions. PV panels convert sunlight directly into electricity using the photovoltaic effect, where semiconductor materials generate electrical charges when exposed to light [7]. These systems are scalable, ranging from small residential rooftop installations to large utility-scale solar farms. The modular nature of PV technology allows for flexible deployment across various settings. CSP systems, on the other hand, use mirrors or lenses to concentrate sunlight onto a small area, producing

☆ This article is part of a special issue entitled: 'Decarbonising Built Env' published in Energy & Buildings.

* Corresponding author.
E-mail address: Moslem.sharifishourabi@ontariotechu.net (M. Sharifishourabi).

https://doi.org/10.1016/j.enbuild.2025.115907
Received 18 January 2025; Received in revised form 5 March 2025; Accepted 20 May 2025
Available online 21 May 2025

Nomenclature

C_P	Specific Heat (kJ/kgK)
ex	Specific Exergy (kJ/kg)
$\dot{E}x$	Exergy Rate (kW)
$\dot{E}xd$	Exergy Destruction Rate (kW)
h	Specific Enthalpy (kJ/kg)
$\dot{m}$	Flow Rate of Mass (kg/hr)
P	Pressure (kPa or bar)
$\dot{Q}$	Heat Transfer Rate (kW)
R	Ideal Gas Constant
s	Specific Entropy (kJ/kgK)
T	Temperature (°C*or*K)
$\dot{W}$	Work Rate (kW)
y	Mole Fraction of Component (%)

Greek Letters

η	Energy Efficiency (%)
Ψ	Exergy Efficiency (%)
E	Energy Interaction Parameter for Component (J/mol)

Subscripts

0	Reference
1,2,3, …	Thermodynamic State Points
Abs	absorption
Ch	Chemical
COMP	Compressor
COND	Condenser
DECOMP	Decomposition Unit
H	Heliostat
HEX	Heat Exchanger
In	Inlet
Out	Outlet
Pyro	Pyrolysis
Rec	Receiver
S	Solar, Source, Stream
SRC	Steam Rankine Cycle
TES	Thermal Energy Storage

Superscripts

ch	Chemical
ph	Physical

Acronyms

BTO	Biomass To Olefins
CCHP	Combined Cooling, Heating, and Power
ch	Chemical
COND	Condenser
COP	Coefficient of Performance
CSP	Concentrated Solar Power
EES	Engineering Equation Solver
FC	Fuell Cell
HEX	Heat Exchanger
hr	Hour
ICE	Internal Combustion Engine
in	Inlet
LHV	Lower Heating Value
LPG	Liquefied Petroleum Gas
MTP	Methanol-to-Propylene
ORC	Organic Rankine Cycle
out	Outlet
PV	Photovoltaic
PVHP	Photovoltaic-based Hydrogen Production
SRC	Steam Rankine Cycle
TES	Thermal Energy Storage

high temperatures that generate steam to drive turbines for electricity production [8]. Despite its advantages, solar energy faces challenges, including variability due to weather conditions and the day-night cycle. Advancements in energy storage technologies are essential to store excess energy produced during sunny periods for use during low-sunlight conditions, thereby enhancing grid reliability and resilience.

Beyond solar energy, biomass energy emerges as a versatile and promising solution for both energy generation [9] and effective waste management [10]. Biomass refers to organic materials that can be converted into bioenergy, including municipal solid waste, agricultural residues such as crop stalks and husks, forestry by-products like wood chips and sawdust, and food waste from households or industries [11]. These materials serve as feedstocks for energy production processes, providing a renewable and often underutilized resource. Biomass can be converted into bioenergy through several methods, each offering unique benefits and applications. Combustion is one of the most established methods, directly burning biomass to produce heat and power. Anaerobic digestion involves the breakdown of organic materials in an oxygen-free environment [12]. This results in biogas, a mixture of methane and carbon dioxide, that can be used as a fuel for heating or electricity generation. Gasification, on the other hand, converts biomass into syngas (a mixture of carbon dioxide and hydrogen) through a high-temperature process, which can then be utilized for electricity generation or as a chemical feedstock [13]. Among the diverse applications of biomass, one particularly innovative and beneficial approach is the production of biochar [14]. Biochar is a carbon-rich material obtained through the pyrolysis of organic waste essentially, the thermal decomposition of biomass in the absence of oxygen. This process not only captures carbon, effectively sequestering it and preventing its release into the atmosphere as a greenhouse gas, but also yields biochar that has valuable agricultural applications. When applied to soil, biochar improves its health by enhancing nutrient content [15], increasing water retention capacity, and promoting beneficial microbial activity. These soil enhancements contribute to improved crop yields and overall agricultural sustainability, making biochar a multifaceted tool in addressing climate change and supporting ecological resilience. Biochar sequesters carbon, preventing its release into the atmosphere as greenhouse gas, and enhances soil health by improving nutrient content and water retention.

The shift to renewable energy sources must be accompanied by innovative approaches to energy generation and utilization in decarbonized buildings [16]. Integrated energy systems, which combine multiple energy generation processes, significantly boost efficiency [17]. Traditional single-generation systems [18], typically produce only one form of energy, often electricity, leading to substantial energy losses. In contrast, cogeneration systems, or combined heat and power systems, generate both electricity and useful heat from a single energy source, reducing waste and improving efficiency. Trigeneration systems take this concept further by producing electricity, heat, and cooling from the same source, enhancing versatility and efficiency [19]. For example, Jia and Paul [20], evaluated a combined cooling, heating, and power (CCHP) system that integrated a biomass gasifier, a Stirling engine, an internal combustion engine (ICE), and an absorption chiller. Stirling engine improved power output by 14 % and helped achieve a net electrical efficiency of 37 % and a total efficiency of over 60 %. The ICE reached a thermal efficiency of 39 % at 5000 rpm. Recycling the weak solution in the absorber enhanced the absorption chiller's COP by 7 %, reaching 76 %.

Advanced multigeneration systems push the boundaries even more, enabling the production of additional outputs like desalinated water, biofuels, or hydrogen [21]. These systems optimize resource use, minimize energy waste, and mitigate environmental impacts, marking a crucial step towards a sustainable energy future. For instance, Meng et al. [22], conducted an energy and exergy analyses of a wind-hydrogen coupled polygeneration system. By utilizing waste heat in multiple stages, the system enhanced electricity, hydrogen, and heat production while improving equipment operation. Increasing the fuel cell (FC) operating temperature raised the exergy efficiency of the FC-ORC and the system to 51.91 % and 58.83 %, respectively, while higher hydrogen storage pressure improved exergy efficiency by 6.87 %, resspectively.

Energy storage systems has a critical role in the transition toward sustainable energy solutions by addressing the challenges of intermittent energy supply from renewable sources [23]. These systems store surplus energy when production exceeds usage and deliver it when production is insufficient, ensuring a steady energy supply. Among the various energy storage options, thermal energy storage (TES) systems have garnered significant attention for their ability to store heat or cold for later use [24]. TES systems operate by capturing and storing energy in the form of heat, either as sensible heat (in materials like molten salts or water), latent heat (employing phase-change materials), or through thermochemical processes [25]. These systems are particularly effective for applications such as district heating, solar thermal power plants, and industrial processes, as they can balance energy supply and demand over hours, days, or even seasons. By integrating TES with renewable energy sources, such as solar thermal systems, one can enhance energy efficiency, reduce reliance on fossil fuels, and pave the way for a more sustainable energy infrastructure [26]. For example, Gao [27] employed energy storage systems utilizing solar-assisted supercritical compressed carbon dioxide to evaluate their performance. Two systems were proposed: one used a simple regenerative compression cycle, and the other utilized a recompression cycle. Thermodynamic and economic analyses revealed that these systems achieved higher energy efficiency and solar-electricity conversion rates compared to baseline systems, with efficiencies of 23.56 % and 28.77 %, respectively. The following are recent articles on renewable energy system developments.

Meng et al. [22] conducted an energy and exergy analyses of a wind-hydrogen coupled polygeneration system. They utilized waste heat through multistage processes to improve energy output and equipment efficiency. The study evaluated the effects of parameters such as operating temperatures and hydrogen storage pressure on exergy efficiency and destruction. The results showed that increasing fuel cell operating temperature significantly enhanced the system's efficiency, reaching 58.83 %. The economic evaluation revealed a static payback period of 7.3 years for the system.

In a study by Budovich [28], an energy system using biomass was analyzed for concurrent power and hydrogen production. The system, powered by biomass combustion, included an organic Rankine cycle (ORC) with a feed fluid heater and heat recovery exchanger for dual generation. Various ORC configurations and working fluids were examined using thermodynamic models, with R113 showing the highest energy and exergy efficiencies at 67.15 % and 3.69 %, respectively.

Sharifishourabi et al [29] developed a solar energy-based multigeneration system designed to meet the energy needs of sustainable communities. The system integrated a solar subsystem, a steam Rankine cycle, a Rankine cycle with reheat, a double-effect absorption system, and an electrolyzer to efficiently produce electricity, heating, cooling, and hydrogen. Their study included environmental, energy, and exergy performance analyses. The system achieved energy and exergy efficiencies of 53.32 % and 48.28 %, respectively. Additionally, it demonstrated the capability to prevent 332.7 kg of CO_2 emissions per MWh of electricity. The findings highlighted the system's efficiency and environmental benefits, emphasizing its potential to mitigate climate change impacts. In a study by Chen et al. [30], biomass and solar energy were used to propose a novel system for carbon-negative production of olefins and green hydrogen. The system included biomass-to-olefins (BTO) and photovoltaic-based hydrogen production (PVHP). Solar energy was utilized to convert excess carbon dioxide into olefins, achieving zero emissions during production. Researchers analyzed five types of biomasses and conducted energy, exergy, and techno-economic evaluations in three cities in China. Their study showed that the system could produce 4550–5500 tons of ethylene and propylene annually with energy efficiencies of 55–65 %.

Hao et al. [31] developed a biomass CO_2 gasification system to achieve near-zero emissions and high-efficiency combined cooling, heating, and power generation. The system used CO_2 as an auxiliary gasification agent to improve coke conversion and increase the calorific value of syngas. The thermodynamic model showed a maximum energy efficiency of 70.2 %, a net electrical efficiency of 50.41 %, and a CO_2 capture rate of 99.9 %, with specific emissions as low as 0.64 kg/MWh. Sharifishourabi et al. [32], developed a system that integrated hydrogen production and energy storage to meet variable residential energy demands by utilizing solar and geothermal energies. The system combined multiple technologies, including a steam Rankine cycle, an ammonia-water-based double-effect absorption system, two organic Rankine cycles, thermal energy storage, battery and hydrogen storage, and a sonohydrogen production device. They analyzed the system using energy and exergy approaches and found it could produce 0.0016 kg/s of hydrogen, generate 2177 kW of net output, supply 4337 kW for heating, and provide 903.8 kW of cooling capacity. The energy and exergy efficiencies were 83.28 % and 58.71 %, respectively, with energetic and exergetic COP values of 1.646 and 0.6215. Alarnaot-Alarnaout et al. [33] studied a high-temperature heat pump using R-1234ze, designed for district heating and cooling networks. They tested its performance with and without an internal heat exchanger and found that the internal heat exchanger improved heating capacity by up to 19.3 % and increased the COP by 15.6 % for high condensing temperatures. Their findings emphasized the potential of heat pumps in reducing CO_2 emissions and supporting decarbonized buildings by replacing fossil fuel-based heating systems.

Despite significant advancements in renewable energy systems, the literature reveals a notable gap in clean and sustainable propane production technologies. Existing studies primarily focus on single or dual-generation systems, often neglecting the potential for integrated multi-generation setups that include propane as a key output. Furthermore, conventional propane production methods heavily rely on fossil fuels, contributing to significant greenhouse gas emissions. While some research explores biomass and solar energy integration, these efforts typically emphasize electricity, hydrogen, or heat production, with limited attention to propane synthesis. This highlights the need for innovative approaches that combine renewable energy sources, advanced thermal energy storage, and efficient thermochemical processes to achieve clean and sustainable propane production. The building sector represents a critical area where clean propane can be utilized effectively. Current energy systems for heating and cooling in buildings often rely on fossil fuels, which adds to the sector's carbon footprint. Integrating renewable propane into building applications can support decarbonization efforts while ensuring reliable energy supply. Additionally, the building sector offers substantial opportunities for deploying advanced thermal energy storage systems to optimize energy use and reduce emissions. The current study develops a novel integrated solar-biomass system coupled with thermal energy storage designed for the simultaneous production of electricity, heat, hydrogen, and propane, addressing the critical gap in clean propane production technologies. The system uniquely uses solar energy through a steam Rankine cycle and biomass pyrolysis, enhanced with advanced thermal management. Key innovations include the integration of multigeneration capabilities, detailed thermodynamic analysis to evaluate energy and exergy efficiencies, and parametric studies to optimize system performance. By addressing critical challenges in renewable energy integration and clean propane synthesis, this study aims to establish a comprehensive

framework for efficient, low-carbon energy generation and versatile resource utilization, with special emphasis on the building sector. Clean propane has the potential to transform heating, cooling, and energy systems in buildings, supporting global sustainability initiatives and reducing greenhouse gas emissions.

2. System Description

The energy system, as illustrated in Figs. 1–3, integrates several advanced and interconnected subsystems to develop a sustainable and efficient energy framework for building sector. These subsystems include solar and biomass energy systems, thermal energy storage, a steam Rankine cycle (SRC), and a propane production process. Each component and sub-system contributes to achieving high efficiency, sustainability, and environmental benefits.

The system benefits energy from both renewable solar and biomass sources, ensuring a diverse and reliable supply. Solar energy is concentrated using a heliostat field and transmitted to a central receiver, producing high-temperature thermal energy at approximately 700 °C. Biomass, particularly municipal and food waste, is used in a pyrolysis process to generate syngas and biochar at an operating pressure of 100 kPa, further diversifying the energy input.

A key feature of the design is its thermal energy storage units, consisting of hot and cold thermal energy storage tanks. The hot TES operates at temperatures of up to 700 °C to store thermal energy generated from solar or biomass inputs, which the TES system primarily relies on sensible heat storage. The cold TES operates at lower temperatures, maintaining a balance between energy supply and demand. These units provide energy buffering to maintain a consistent energy supply during periods of low solar irradiance or peak energy demand. This ensures reliable energy output and improves system resilience against environmental variability. The TES drives the steam Rankine cycle.

The SRC is a central component of the system, converting thermal energy into heat and electricity. In this cycle, high-pressure steam is generated at 10,000 kPa and temperatures of 581 °C before being expanded through turbines to produce electricity. The cycle is designed to achieve optimal efficiency by utilizing both high and intermediate pressure stages. The steam exiting the turbine is condensed at lower pressures (around 215 kPa) and recycled, supporting cogeneration by supplying heat to community.

The propane production process in this system is an innovative and environmentally friendly approach that utilizes renewable energy inputs from both solar and biomass sources. This integrated system efficiently transforms waste and renewable resources into clean propane while minimizing environmental impacts. The process begins with the pyrolysis of municipal and food waste, which operates at a high temperature of 700°C and a pressure of 5000 kPa. During pyrolysis, organic waste is thermally decomposed in the absence of oxygen, producing syngas (a mixture of CO_2 and H_2) and biochar. The biochar, a byproduct generated at 471 °C, is a valuable material that can enhance soil fertility or be used as a carbon sink, supporting sustainable agriculture and waste management practices. The syngas is then directed to a methanol synthesis unit. In this stage, CO and H_2 are catalytically converted into methanol at elevated pressures and temperatures. This process is crucial as methanol serves as the intermediate feedstock for downstream propane production. The methanol produced is then fed into a Methanol-to-Propylene (MTP) conversion unit. Using advanced catalytic processes, methanol undergoes dehydration and oligomerization reactions to form propylene (C_3H_6). This stage occurs in specialized reactors operating under carefully controlled conditions to maximize propylene yield while minimizing side reactions. In the final step, the propylene is hydrogenated in the Propylene Hydrogenation. During this process, hydrogen (H_2) reacts with propylene (C_3H_6) to form propane (C_3H_8). This reaction is facilitated by a metal-based catalyst under high pressures and moderate temperatures. The propane produced is then cooled and stored in pressurized tanks to ensure safe and efficient distribution.

The utilization of municipal and food waste not only mitigates landfill accumulation but also serves as a renewable energy resource. The pyrolysis process converts waste into clean energy products, including syngas and biochar, reducing greenhouse gas emissions and supporting circular economy principles. Pyrolysis reactors operate at high temperatures, reaching up to 700 °C, to ensure efficient waste conversion.

The combined functionality of the SRC, TES, and propane production units results in a system that is versatile and adaptive. The energy system achieves sustainability by reducing dependency on fossil fuels through renewable energy integration, minimizing greenhouse gas emissions with clean energy production, enhancing energy security and reliability through TES, and contributing to waste reduction and resource efficiency via the pyrolysis process. With steam pressures ranging from 10,000 kPa in high-pressure stages to 215 kPa during condensation, and with thermal storage temperatures varying between 700 °C (hot storage) and lower levels in cold storage, the system is optimized for efficiency. This ability to dynamically handle variations in temperature and pressure ensures its operational robustness and energy efficiency.

3. Thermodynamic analysis and assessment

In this section, the equations related to the major segments of the thermodynamic analysis and modeling of energy systems are provided. These equations cover various renewable energy sources, including solar towers, biomass, and other critical components like turbines, heat exchangers, pumps, and condensers. The aim is to offer a systematic framework for evaluating the performance of these systems using both energy and exergy analyses, allowing for a deeper understanding of efficiency, energy utilization, and potential system optimizations [34]. The following assumptions are considered in this study: the reference temperature is assumed to be 25 °C, and atmospheric pressure is considered as 100 kPa. All processes operate under steady-state conditions, with heat losses from thermal energy storage tanks and pipelines assumed negligible. The specific heats of gases and working fluids are considered constant over the operating temperature range, and ideal gas behavior is assumed for all gaseous components in the system. The heliostat field operates with an average optical efficiency of 75 %. Thermal and mechanical losses in the turbine and pumps are accounted for, with the turbine's efficiencies assumed at 85 %. Pyrolysis temperature and pressure are set at 700 °C and 5000 kPa, respectively. The thermal energy storage units are perfectly insulated, with no thermal degradation of the storage media occurring.

Solar towers represent a highly efficient form of concentrated solar power technology, where heliostats (mirrors) focus sunlight onto a central receiver, which absorbs the solar radiation and converts it into heat. This heat is then used to produce electricity through thermodynamic cycles. The system's efficiency depends on multiple factors, including the rate of heat capture by the receiver, the performance of the heliostats, and the overall energy and exergy efficiencies of the components. Key equations related to the solar tower section, including those describing heat capture, absorption, and efficiencies, are summarized in Table 1.

The equations listed in Table 1 form the foundation for analyzing the performance of solar tower systems, with particular focus on heliostat and receiver efficiencies. By optimizing these parameters and minimizing losses, solar tower systems can significantly enhance their energy conversion efficiency, making them a promising solution for large-scale renewable energy generation.

Biomass has emerged as a key renewable energy source due to its abundance, sustainability, and potential to reduce greenhouse gas emissions. It is a complex mixture of organic materials, including carbon (C), hydrogen (H), oxygen (O), nitrogen (N), sulfur (S), and trace elements such as chlorine (Cl), with the composition varying based on the source and type of biomass. The thermodynamic properties of biomass

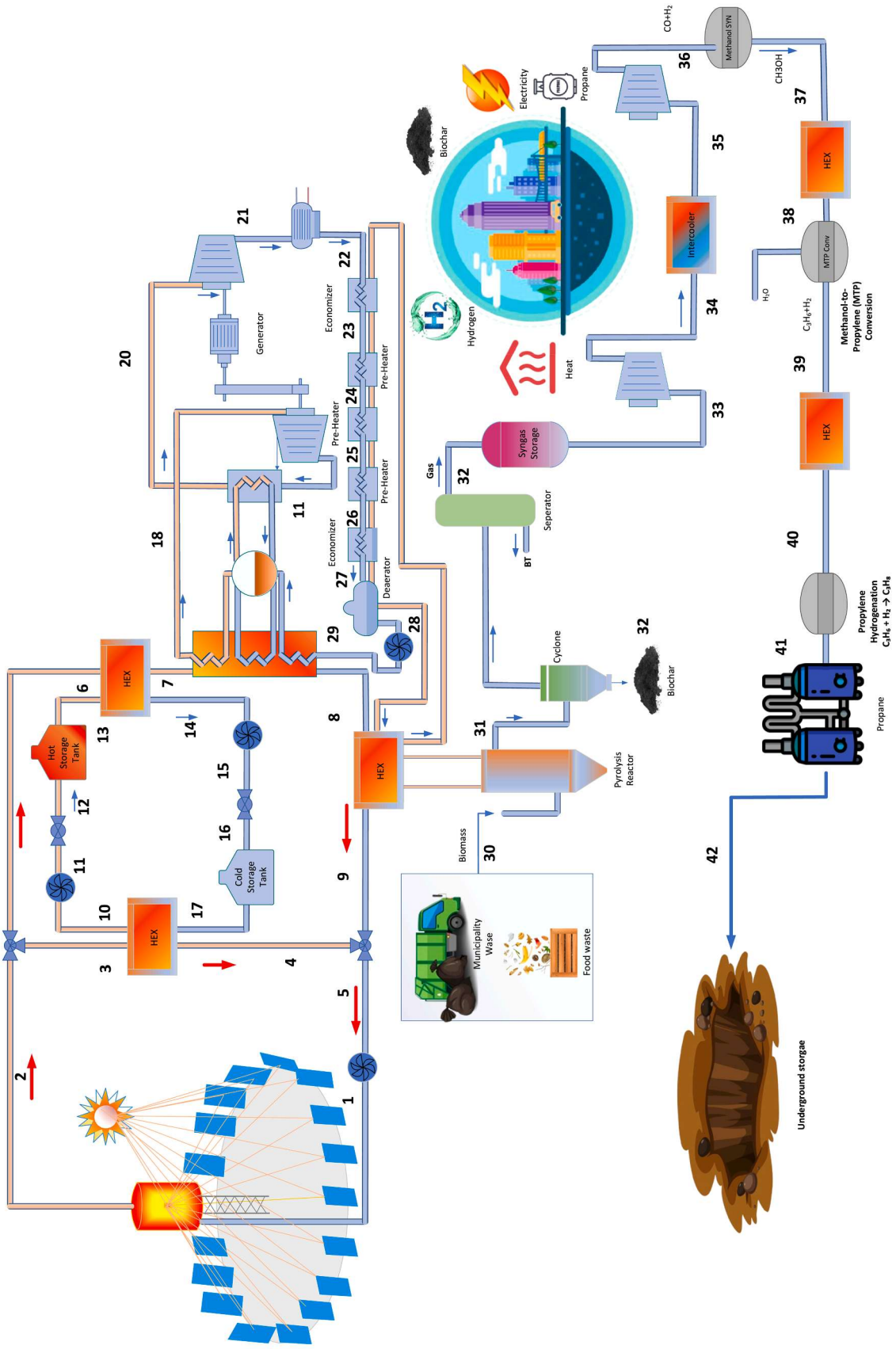

Fig. 1. A schematic diagram of the currently developed energy system for buildings.

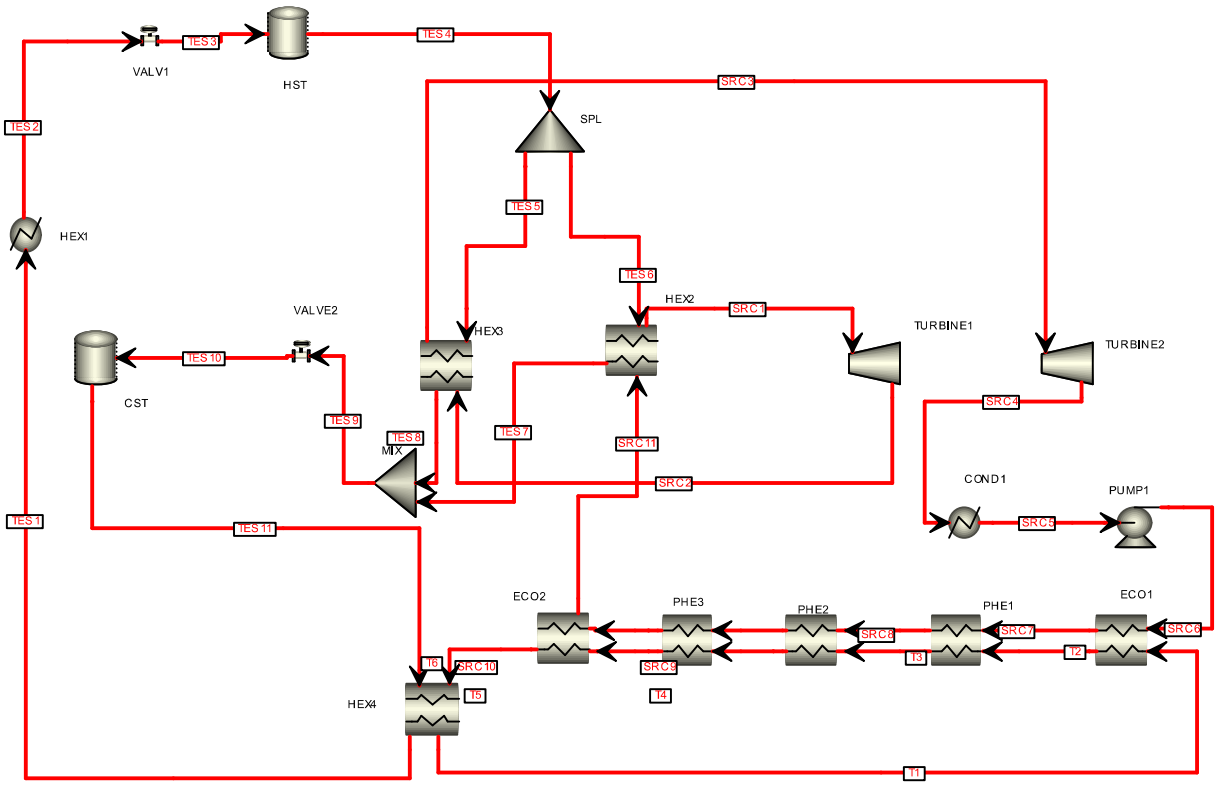

Fig. 2. The Aspen Plus simulation layout of the top sub-system of the developed system.

are essential for understanding its potential as an energy source and for optimizing processes like pyrolysis, gasification, and combustion. To assess the efficiency of energy conversion processes involving biomass, exergy analysis is a powerful tool. Note that exergy quantifies the quality or usability of energy, distinguishing between the usable and unusable portions of energy in a system. This includes both chemical exergy, related to the intrinsic energy stored in the chemical bonds of the biomass, and physical exergy, derived from temperature and pressure deviations from a reference state. The chemical exergy of biomass can be expressed through empirical relationships based on its elemental composition. For example, Eq. (1) provides a formula to calculate the chemical exergy of organic streams as a function of the mass fractions of carbon (C), hydrogen (H), nitrogen (N), sulfur (S), oxygen (O), and ash (A) [35]:

$$ex^{ch} = 362.0083C + 1101.841H + 2.418N + 196.701S - 86.218O - 21.1A \quad (1)$$

In addition to chemical exergy, the specific physical exergy of organic streams can be calculated using Eq. (2):

$$ex^{ph} = C_p\left((T - T_0) - T_0 ln\left(\frac{T}{T_0}\right)\right) \quad (2)$$

For gas streams, the total exergy is the sum of physical and chemical exergies. The physical exergy for gases is given in Eq. (3), while chemical exergy is calculated in Eq. (4):

$$ex^{ph} = C_p\left((T - T_0) - T_0 ln\left(\frac{T}{T_0}\right)\right) + RT_0 ln\left(\frac{P}{P_0}\right) \quad (3)$$

$$ex^{ch} = n\left(\sum_i y_i e_i + RT_0 \sum_i y_i ln(y_i)\right) \quad (4)$$

These exergy formulations allow for a comprehensive analysis of energy transformations in biomass conversion processes. The general energy balance for these processes, accounting for inputs and losses, is expressed in Eq. (5):

$$\dot{m}_{in} ex^{ch}_{in} + \dot{Q}\left(1 - \frac{T_0}{T_{pyrolysis}}\right) = \dot{m}_{out} ex^{ch}_{out} + \dot{m}_{out} ex^{ch}_{out} + \dot{E}xd \quad (5)$$

Table 2 summarizes the elemental composition of a typical biomass sample, highlighting the mass fractions of its major constituents. These values directly influence the chemical exergy and provide insight into the energy potential of the biomass. This detailed breakdown of biomass composition, combined with the exergy analysis framework, forms the basis for evaluating thermochemical conversion processes, ensuring efficient and sustainable energy utilization.

In energy systems, the performance of key components such as turbines, heat exchangers, pumps, and condensers are critical to the overall efficiency and sustainability of the process. Energy and exergy analyses provide complementary perspectives for evaluating these components. While energy analysis considers the conservation of energy, exergy analysis accounts for energy quality and identifies irreversibilities within the system. According to the assumptions, the general thermodynamic equations for this study are provided as follows [34]:

Mass balance equation:

$$\sum_{in} \dot{m}_{in} = \sum_{out} \dot{m}_{out} \quad (6)$$

Energy balance equation:

$$\sum_{in} \dot{Q}_{in} + \sum_{in} \dot{W}_{in} + \sum_{in} \dot{m}_{in}(h_{in}) = \sum_{out} \dot{Q}_{out} + \sum_{out} \dot{W}_{out} + \sum_{out} \dot{m}_{out}(h_{out}) \quad (7)$$

Exergy balance equation:

$$\sum_{in} \dot{E}x_{\dot{Q}_{in}} + \sum_{in} \dot{W}_{in} + \sum_{in} \dot{m}_{in} ex_{in} = \sum_{out} \dot{E}x_{\dot{Q}_{out}} + \sum_{out} \dot{W}_{out} + \sum_{out} \dot{m}_{out} ex_{out} + \dot{E}x_d \quad (8)$$

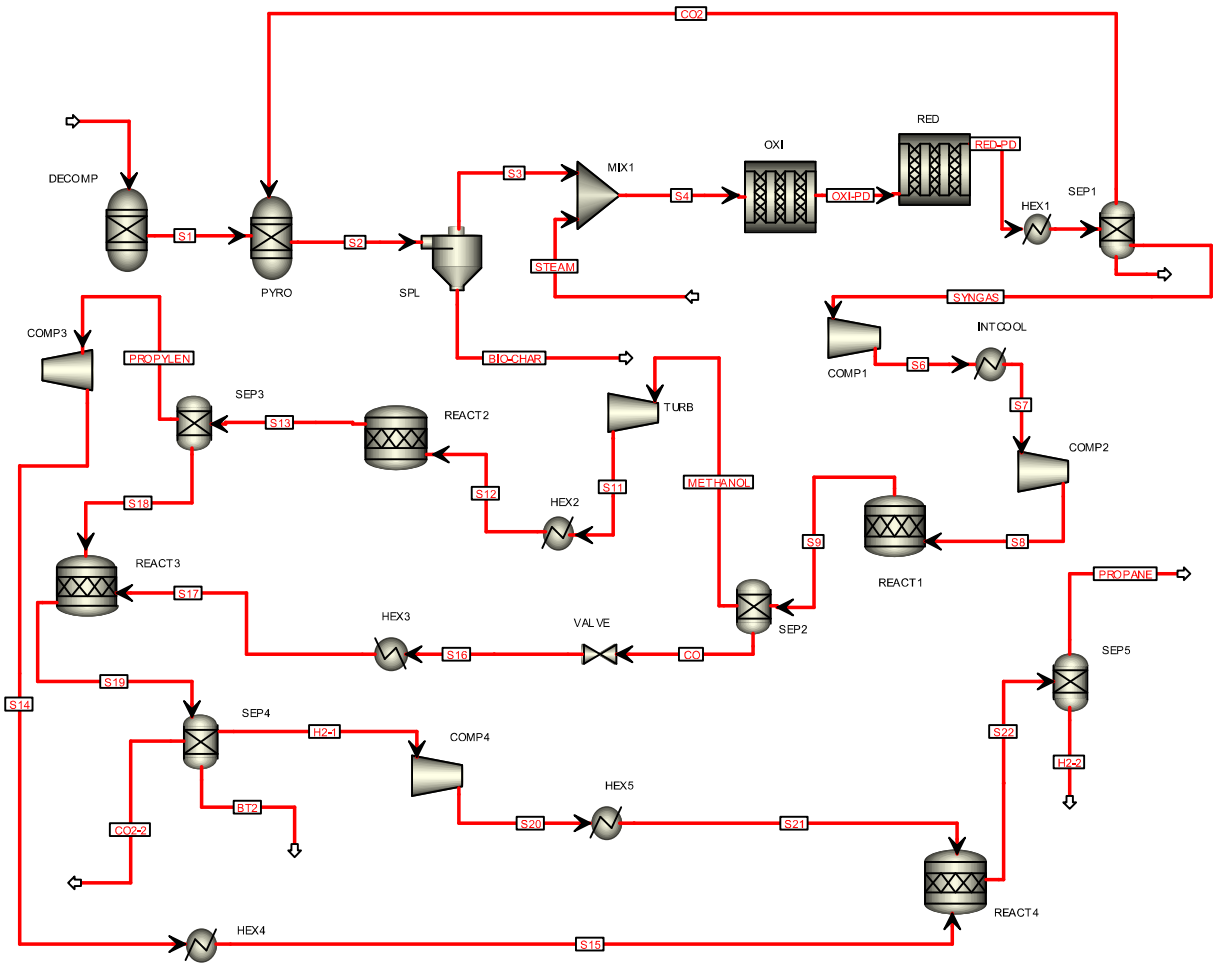

Fig. 3. The Aspen Plus simulation layout of the bottom sub-system of the developed system.

Table 1
The solar tower related thermodynamic equations.

Equation	Description
$\dot{Q}_{rec}=\eta_h \dot{Q}_s$	Heat captured by the receiver.
$\dot{Q}_s=IA_{field}$	Heat absorption rate from solar radiation.
$\dot{Q}_{rec}=\dot{Q}_{rec,abs}+\dot{Q}_{total\,loss}$	$\dot{Q}_{rec,abs}$ and $\dot{Q}_{total,\,loss}$ represent the rates of total heat absorbed and heat losses in the receiver, respectively.
$\eta_h=\frac{\dot{Q}_{rec,abs}}{\dot{Q}_s}$	Heliostat energetic efficiency
$\psi_h=\frac{\dot{E}x_{rec,abs}}{\dot{E}x_s}$	Heliostat exergetic efficiency
$\eta_{rec}=\frac{\dot{Q}_{rec,abs}}{\dot{Q}_{rec}}$	Receiver energetic efficiency
$\eta_{rec}=\frac{\dot{Q}_{rec,abs}}{\dot{Q}_{rec}}$	Receiver exergetic efficiency

Table 2
The biomass composition and their mass fraction values (compiled from Opatokun et al. [35]).

Element	Mass Fraction (%)
C	54.18
H	5.37
O	31.7
N	1.28
S	0.20
CL	0.13
Ash	7.14

These equations form the basis for evaluating component efficiencies, diagnosing system losses, and improving the performance of energy conversion systems. By identifying and minimizing exergy destruction, the overall efficiency of the system can be enhanced, contributing to more sustainable energy utilization.

The overall energy and exergy efficiencies are provided below.

$$\eta_{System}=\frac{\sum\left(\dot{m}_i LHV_i\right)+\dot{W}_{net}+\dot{Q}_{useful}}{\dot{m}_{biomass}LHV_{biomass}+\dot{Q}_{solar}} \tag{9}$$

where η_{System} is overall energy efficiency of the system, $\sum\left(\dot{m}_i LHV_i\right)$ is chemical energy of fuel products, $\dot{W}_{net}$ is net electrical work, $\dot{Q}_{useful}$ is useful heat output, $\dot{m}_{biomass}LHV_{biomass}$ is energy from biomass and $\dot{Q}_{solar}$ is solar energy.

$$\psi_{System}=\frac{\sum\left(\dot{m}_i e_{ch,i}\right)+\dot{W}_{net}+\dot{E}x_{usefulheat}}{\dot{m}_{biomass}e_{ch,biomass}+\dot{E}x_{solar}} \tag{10}$$

where ψ_{System} is overall exergy efficiency of the system, $\sum\left(\dot{m}_i e_{ch,i}\right)$ is chemical exergy of fuel products, $\dot{W}_{net}$ is net electrical work, $\dot{E}x_{usefulheat}$ is exergy of useful heat exported, $\dot{m}_{biomass}e_{ch,biomass}$ is chemical exergy of biomass and $\dot{E}x_{solar}$ represents the exergy of the heat received from solar radiation [34].

$$\dot{E}x_{usefulheat} = \dot{Q}_{useful}\left(1 - \frac{T_0}{T_S}\right) \quad (11)$$

4. Results and discussion

The performance of the integrated solar-biomass energy system was evaluated under varying operating conditions to determine its energy and exergy efficiencies, as well as production rates of hydrogen and propane. The optimization is conducted using the Genetic Algorithm (GA) tool in the Engineering Equation Solver (EES), and the optimal values are presented in Table 3. The subsystem of the system is compared with and verified against studies in the literature [36]. Particularly, the Rankine cycle has an energy efficiency of 22.36 %, which is slightly higher than the 20.43 % reported in the study [37].

The integrated solar-biomass energy system demonstrated robust performance under varying operational conditions. The energy efficiency of the system is determined to be 65.7 %, while the exergy efficiency is calculated at 64.6 %. These values indicate the system's capability to effectively utilize the input energy and maintain performance with minimal energy losses. The close alignment between energy and exergy efficiencies reflects the system's thermodynamic efficiency in converting resources into useful outputs. The production capacity of the integrated system encompasses multiple outputs, showcasing its multifunctional potential (see Fig. 4). The system predominantly generates heat, with an output of 9518 kW, indicating its primary role as a heat source. Additionally, it produces 1688 kW of net power and 1094.29 kg/hr of propane, highlighting its versatility in delivering secondary energy products. Furthermore, the system generates hydrogen at a rate of 49.02 kg/hr, contributing to the sustainable production of a clean energy carrier. This diverse production profile underscores the system's efficiency and capability to meet various energy demands.

4.1. Effect of thermal energy storage temperature on the system efficiencies and output capacities

Thermal energy storage plays a critical role in maintaining energy output stability and enhancing system performance. The analysis investigates the impact of TES temperature variation on both system efficiencies and production rates of hydrogen and propane. This evaluation highlights the interplay between thermal management and output optimization. To better understand the dynamics of this relationship, the TES temperature was varied incrementally between 600 °C and 700 °C. The results provide insights into the optimal operating conditions for maximizing the system's efficiency and production outputs. The interplay between TES temperature, system performance, and individual product yields reveals critical trends.

Fig. 5 illustrates the impact of thermal energy storage system temperature on the production rates of hydrogen and propane, showcasing the results of advancements in energy system development. The data reflects the interplay between the thermal energy storage system's temperature and the output rates of these two gases, which are key products in the energy process. As the temperature of the thermal energy storage system increases from 600 °C to 700 °C, a distinct trend is observed. The production rate of hydrogen exhibits a gradual decrease, from 52.40 kg/hr at 600 °C to 49.02 kg/hr at 700 °C. Conversely, propane production demonstrates a steady increase within the same temperature range, starting at 1072.53 kg/hr at 600 °C and rising to 1094.29 kg/hr at 700 °C. This behavior is attributed to the thermodynamic characteristics and reaction mechanisms of the energy system. Meanwhile, the increase in propane production suggests enhanced synthesis or improved yield dynamics under elevated thermal conditions.

Fig. 6 illustrates the relationship between the temperature of the thermal energy storage system, the net work rate, and heat production.

Table 3
The values of each state point as obtained from the EES.

Stream name	Mass flows (kg/hr)	Temperature (°C)	Pressure (bar)	Specific enthalpy (kJ/kg)
BIO-CHAR	1212.23	700.00	1.01	769.30
BT	140.41	25.00	0.81	−2323.24
BT2	408.10	500.00	1.00	−12482.36
CO	1409.33	348.00	81.00	−3603.02
CO2	4749.06	25.00	0.81	−8942.18
CO2-2	2214.33	500.00	1.00	−8454.44
FEED	5000.00	700.00	1.01	−3643.18
H2-1	101.43	500.00	1.00	6898.24
H2-2	52.40	150.00	10.00	1807.67
METHANOL	2338.03	348.00	81.00	−5837.22
OXI-PD	8636.84	800.00	1.00	−5160.94
PROPANE	1072.53	150.00	10.00	−2146.12
PROPYLEN	1023.50	500.00	1.00	1585.48
RED-PD	8636.84	800.00	1.00	−5302.33
S1	5000.00	700.00	1.01	−67.23
S11	2338.03	63.72	1.00	−6225.76
S12	2338.03	500.00	1.00	−5354.26
S13	2338.03	500.00	1.00	−6323.98
S14	1023.50	641.93	10.00	2031.19
S15	1023.50	150.00	10.00	687.69
S16	1409.33	348.71	1.00	−3603.02
S17	1409.33	500.00	1.00	−3434.70
S18	1314.53	500.00	1.00	−12482.36
S19	2723.86	500.00	1.00	−8486.07
S2	9749.06	700.00	1.01	−4501.00
S20	101.43	1286.60	10.00	18968.51
S21	101.43	150.00	10.00	1807.67
S22	1124.93	150.00	10.00	−1954.64
S3	8536.84	700.00	1.01	−5249.38
S4	8636.84	698.43	1.00	−5330.61
S5	8636.84	25.00	0.81	−6531.20
S6	3747.36	347.51	8.13	−2953.75
S7	3747.36	25.00	8.13	−3637.40
S8	3747.36	347.96	81.30	−2946.01
S9	3747.36	348.00	81.00	−4966.87
SRC1	14400.00	580.87	100.00	−12409.98
SRC10	14400.00	221.23	100.00	−15037.53
SRC11	14400.00	252.23	100.00	−14868.48
SRC2	14400.00	470.39	50.00	−12611.70
SRC3	14400.00	569.21	50.00	−12384.70
SRC4	14400.00	214.67	2.70	−13069.65
SRC5	14400.00	130.00	2.70	−15491.74
SRC6	14400.00	131.23	100.00	−15478.81
SRC7	14400.00	161.23	100.00	−15337.09
SRC8	14400.00	181.23	100.00	−15240.13
SRC9	14400.00	201.23	100.00	−15140.53
STEAM	100.00	600.00	1.00	−12265.57
SYNGAS	3747.36	25.00	0.81	−3636.37
T1	360000.00	380.00	1.00	−12733.66
T2	360000.00	377.24	1.00	−12739.33
T3	360000.00	375.35	1.00	−12743.21
T4	360000.00	373.41	1.00	−12747.19
T5	360000.00	371.40	1.00	−12751.31
T6	360000.00	368.10	1.00	−12758.08
TES1	288000.00	626.65	1.00	−12206.62
TES10	288000.00	640.56	1.50	−12176.11
TES11	288000.00	640.36	1.00	−12176.11
TES2	288000.00	700.00	1.00	−12041.83
TES3	288000.00	700.00	1.00	−12041.83
TES4	288000.00	700.17	1.50	−12041.83
TES5	144000.00	700.17	1.50	−12041.83
TES6	144000.00	700.17	1.50	−12041.83
TES7	144000.00	590.17	1.50	−12287.68
TES8	144000.00	690.17	1.50	−12064.53
TES9	288000.00	640.56	1.50	−12176.11

As the temperature of the thermal energy storage system increases from 600°C to 700°C, both the net work rate and heat production demonstrate a steady upward trend. The net work rate starts at 1688 kW when the storage system temperature is 600°C and increases to 1843 kW at 700°C. Similarly, heat production shows a consistent rise, beginning at 9519 kW

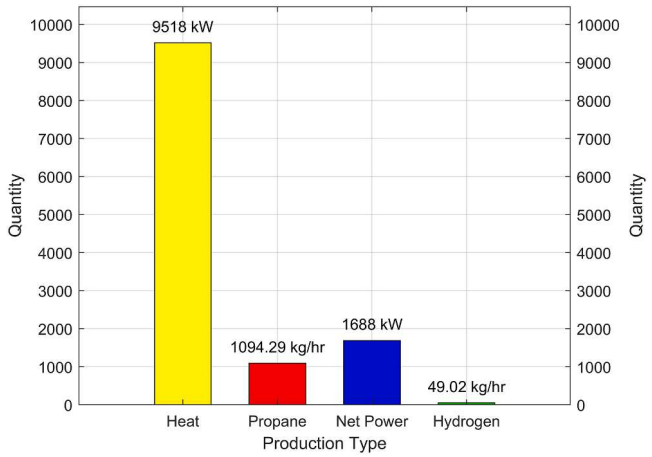

Fig. 4. The production capacities of the system.

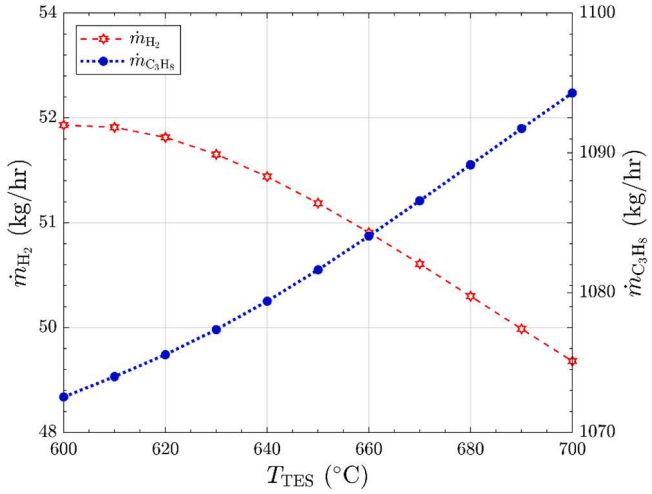

Fig. 5. The effect of variation of thermal energy storage system temperature on hydrogen and propane production.

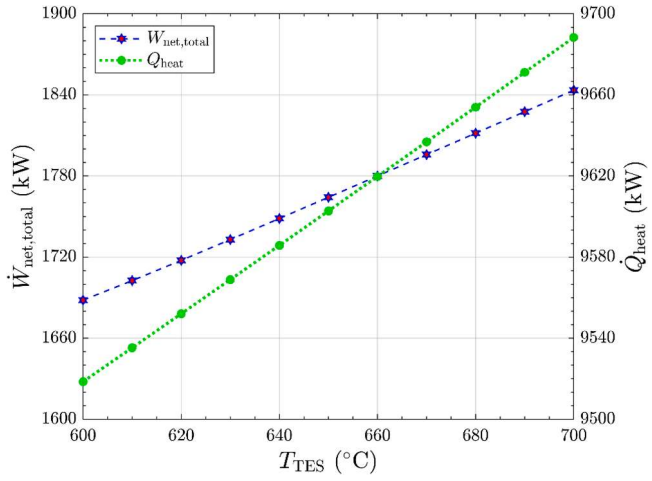

Fig. 6. The effect of variation of thermal energy storage system temperature on useful heat production and work rate.

at 600 and reaching 9688 kW at 700°C. This data highlights the positive correlation between the temperature of the thermal energy storage system and both performance metrics, underscoring the efficiency improvements at higher operating temperatures.

Fig. 7 illustrates the influence of thermal energy storage system temperature on the energy and exergy efficiencies. The results show an increase in both efficiencies as the TES temperature rises, emphasizing the critical role of temperature in optimizing system performance. For energy efficiency, the value increases from 65 % at 600 °C to 65.7 % at 700 °C. Similarly, exergy efficiency shows an improvement, rising from around 63.8 % at 600 °C to 64.6 % at 700 °C. These numerical trends highlight the enhanced system performance achieved with higher TES temperatures. The rise in energy efficiency can be linked to reduced heat losses and better thermal energy utilization at elevated temperatures. Concurrently, the improvement in exergy efficiency reflects a more effective conversion of thermal energy into useful work, as the system operates closer to thermodynamic ideality at higher temperatures.

4.2. *Effect of different parameters on the hydrogen and propane productions*

Fig. 8 presents the effects of varying pyrolysis reactor pressure on hydrogen and propane production rates. The data encompasses pressures from 0.5 to 2.5 bar, specifically at 0.5, 1, 1.5, 2, and 2.5 bar, displaying a clear trend in the production of both gases. For hydrogen, production increases as pressure rises from 0.5 bar, with a mass flow rate of approximately 46.99 kg/hr, peaking at 53.28 kg/hr at a pressure of 1.5 bar, before slightly decreasing to around 52.99 kg/hr at 2.5 bar. Similarly, propane production starts at around 1055.41 kg/hr at 0.5 bar and exhibits a general decline as pressure increases, dropping to about 1041.42 kg/hr at 2.5 bar. However, it is noteworthy that both propane and hydrogen production reach their highest at a pressure of 1 bar, aligning with the primary objective of maximizing propane output in the pyrolysis process.

Fig. 9 presents the effects of variations in inlet steam flow on the production rates of hydrogen and propane. The graph displays two trends: the production rate of hydrogen and the production rate of propane, as functions of the steam mass flow rate, which ranges from 0 to 200 kg/hr. Both hydrogen and propane production rates are shown to increase linearly with the steam mass flow rate. Specifically, hydrogen production rises steadily from approximately 49 kg/hr at 0 steam flow to around 56 kg/hr at the maximum flow rate of 200 kg/hr. Propane production follows an upward trajectory, beginning at 1030 kg/hr and reaching 1115 kg/hr at the highest flow rate. This visualization underscores the direct relationship between steam flow rate and gas production, highlighting the proportional increase in output of both hydrogen and propane with increased steam input.

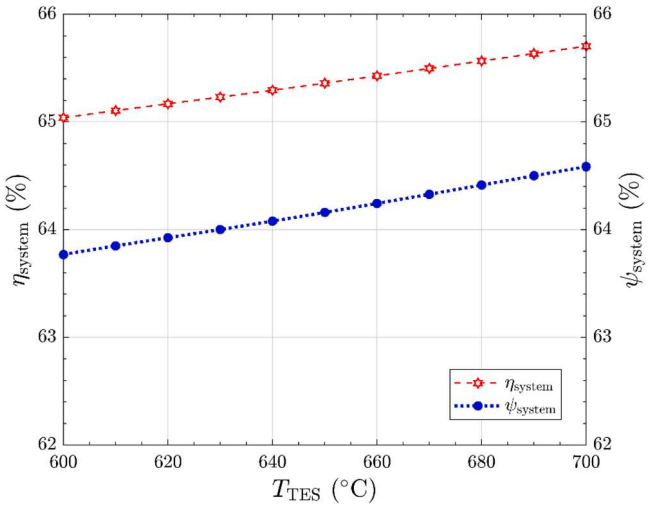

Fig. 7. The effect of variation of thermal energy storage system temperature on the system efficiencies.

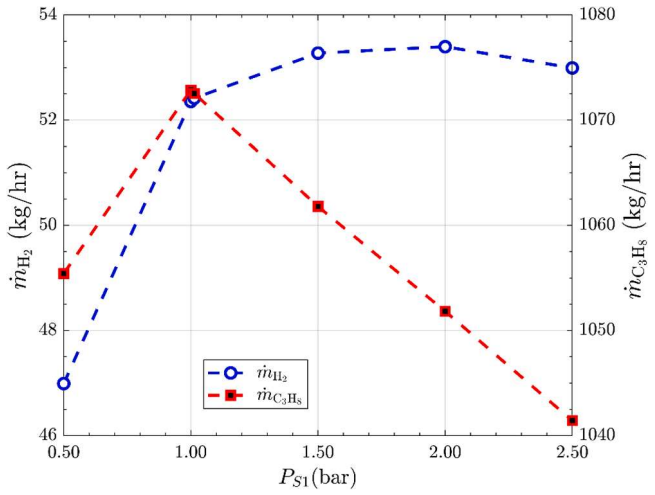

Fig. 8. The effect of variation in pyrolysis reactor pressure on hydrogen and propane production.

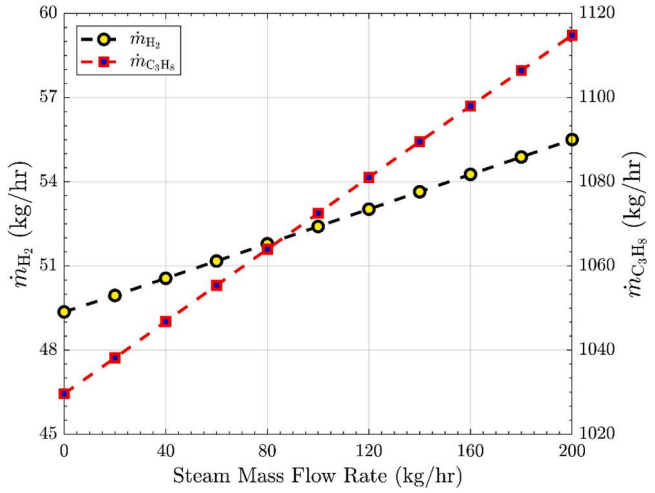

Fig. 9. Effects of variations in inlet steam flow on hydrogen and propane production.

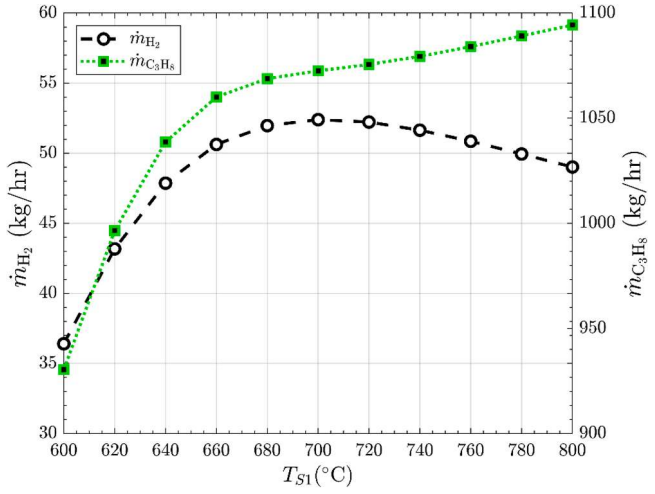

Fig. 10. Effect of variation of pyrolysis unit temperature on the hydrogen and propane production.

Fig. 10 depicts the impact of varying pyrolysis unit temperature on the production rates of hydrogen and propane. The plot traces two distinct curves: one for hydrogen production and another for propane production, over a temperature range from 600 °C to 800 °C. As the temperature increases, hydrogen production exhibits an initial sharp rise, reaching 680 °C, where it stabilizes with minor fluctuations. Beyond 740 °C, there is a slight decline in hydrogen production. In contrast, propane production generally increases with temperature, showing a more gradual and consistent upward trend throughout the same temperature range. This graph illustrates how temperature influences the efficiency and yield of hydrogen and propane in a pyrolysis process, highlighting optimal temperature ranges for maximizing production of each gas.

5. Conclusions

A novel multigeneration renewable energy system is developed to meet community demands for heat, electricity, hydrogen, and propane. The system is modeled using Aspen Plus software and evaluated through thermodynamic analysis. Energy and exergy assessments of the integrated solar-biomass system provide key insights into its performance under varying operating conditions. Increasing the TES temperature from 600 °C to 700 °C improves energy efficiency from 65 % to 65.7 % and exergy efficiency from 63.8 % to 64.6 %. Propane production increases from 1,072.53 kg/hr to 1,094.29 kg/hr, while hydrogen production slightly decreases from 52.40 kg/hr to 49.02 kg/hr. Hydrogen output peaks at 53.28 kg/hr at 1.5 bar, whereas propane production declines from 1,055.41 kg/hr at 0.5 bar to 1,041.42 kg/hr at 2.5 bar. A linear increase in steam flow enhances hydrogen production from 49 kg/hr to 56 kg/hr and propane production from 1,030 kg/hr to 1,115 kg/hr. Hydrogen output reaches its highest level at 680 °C before stabilizing and slightly declining beyond 740 °C, while propane production steadily rises from 600 °C to 800 °C. This study highlights the viability of an integrated solar-biomass system for multigeneration applications. By leveraging renewable energy sources and advanced thermodynamic principles, the system achieves high efficiency and diverse outputs, underscoring its potential to address global energy and environmental challenges. Future studies can explore alternative thermal storage materials, such as phase change materials, to enhance heat retention and efficiency. Additionally, incorporating dynamic simulations to assess time-dependent variations in system performance would provide deeper insights into real-world operation. A techno-economic assessment would also be valuable to validate the system's feasibility and long-term sustainability.

CRediT authorship contribution statement

Moslem Sharifishourabi: Writing – original draft, Visualization, Validation, Software, Resources, Methodology, Investigation, Formal analysis, Data curation. **Ibrahim Dincer:** Writing – review & editing, Supervision, Methodology, Conceptualization. **Atef Mohany:** Writing – review & editing, Supervision, Methodology.

Declaration of competing interest

The authors declare that they have no known competing financial interests or personal relationships that could have appeared to influence the work reported in this paper.

Data availability

Data will be made available on request.

References

[1] H. Liu, Z. Du, T. Xue, T. Jiang, Enhancing smart building performance with waste heat recovery: Supply-side management, demand reduction, and peak shaving via advanced control systems, *Energ. Buildings* 327 (Jan. 2025) 115070, https://doi.org/10.1016/j.enbuild.2024.115070.

[2] S. Christopher, V. Kumaresan, Simulation study of compound parabolic collector-based solar water heating system with thermal energy storage, Energy Storage 4 (3) (2022) e311, https://doi.org/10.1002/est2.311.

[3] M. Afrand, M.S. Targhi, S. Khanmohammadi, Energy and exergy analyses of dual refrigerant system for liquefaction of natural gas, IJEX 31 (1) (2020) 87, https://doi.org/10.1504/IJEX.2020.104726.

[4] T.-I. Ohm, J.-S. Chae, S.-Y. Kim, S.-Y. Kim, S.-H. Moon, Characteristics of a double-swirl combustor for the thermal destruction of waste HFC refrigerants, *International Journal of Global Warming* 15 (4) (Jan. 2018) 413–430, https://doi.org/10.1504/IJGW.2018.093747.

[5] L. Álvarez Flórez, T. Péan, and J. Salom, "Hourly based methods to assess carbon footprint flexibility and primary energy use in decarbonized buildings," *Energy and Buildings*, vol. 294, p. 113213, Sep. 2023, doi: 10.1016/j.enbuild.2023.113213.

[6] K. Elsayed Elfeky, M. Hosny, S. Abu Khatwa, A. Gambo Mohammed, and Q. Wang, "CSP plants cooling technology: Techno-economic analysis, parametric study, and stacking ensemble learning forecasting," *Thermal Science and Engineering Progress*, vol. 54, p. 102777, Sep. 2024, doi: 10.1016/j.tsep.2024.102777.

[7] N. A. A. Mohd Amin and H. F. Mohd Zaid, "A review of hydrogen production using TIO2-based photocatalyst in tandem solar cell," *International Journal of Hydrogen Energy*, vol. 77, pp. 166–183, Aug. 2024, doi: 10.1016/j.ijhydene.2024.05.407.

[8] A. A. Al Kindi, P. Sapin, A. M. Pantaleo, K. Wang, and C. N. Markides, "Thermo-economic analysis of steam accumulation and solid thermal energy storage in direct steam generation concentrated solar power plants," *Energy Conversion and Management*, vol. 274, p. 116222, Dec. 2022, doi: 10.1016/j.enconman.2022.116222.

[9] S.O. Jeje, T. Marazani, J.O. Obiko, M.B. Shongwe, Advancing the hydrogen production economy: A comprehensive review of technologies, sustainability, and future prospects, *Int. J. Hydrogen Energy* 78 (Aug. 2024) 642–661, https://doi.org/10.1016/j.ijhydene.2024.06.344.

[10] A.Y. Goren, A.F. Kilicaslan, I. Dincer, A. Khalvati, Hydrogen production from energetic poplar and waste sludge by electrohydrogenesis using membraneless microbial electrolysis cells, *Renew. Energy* 237 (Dec. 2024) 121750, https://doi.org/10.1016/j.renene.2024.121750.

[11] M. Usman, S. Cheng, S. Boonyubol, J.S. Cross, From biomass to biocrude: Innovations in hydrothermal liquefaction and upgrading, *Energ. Conver. Manage.* 302 (Feb. 2024) 118093, https://doi.org/10.1016/j.enconman.2024.118093.

[12] N. Preuss, F. You, Consequential versus attributional life cycle optimization of poultry manure management technologies in a food-energy-water-waste nexus, *J. Clean. Prod.* 469 (Sep. 2024) 143133, https://doi.org/10.1016/j.jclepro.2024.143133.

[13] M.M. Santos, M.A. Diez, M. Suárez, T.A. Centeno, Innovative particleboard material from the organic fraction of municipal solid waste, *Journal of Building Engineering* 44 (Dec. 2021) 103375, https://doi.org/10.1016/j.jobe.2021.103375.

[14] C.A. Diaz, A.K. Castro, N.J. Cáceres, E.S. Siza, Exergy study of co-firing processes of low-grade coal with oil palm kernel shell (as received, torrefied, and pyrolysed) in a brick furnace, using Aspen Plus, *Int. J. Exergy* 38 (4) (Jan. 2022) 422–441, https://doi.org/10.1504/IJEX.2022.124612.

[15] R. Gautam, N.V. Ress, R.S. Wilckens, U.K. Ghosh, Hydrogen production in microbial electrolysis cell and reactor digestate valorization for biochar – a noble attempt towards circular economy, *Int. J. Hydrogen Energy* 52 (Jan. 2024) 649–668, https://doi.org/10.1016/j.ijhydene.2023.07.190.

[16] J. E. Pachano, C. Nuevo-Gallardo, and C. Fernández Bandera, "An empirical comparison of a calibrated white-box versus multiple LSTM black-box building energy models," *Energy and Buildings*, vol. 333, p. 115485, Apr. 2025, doi: 10.1016/j.enbuild.2025.115485.

[17] T. Jing, Y. Zhao, Optimizing energy consumption in smart buildings: A model for efficient energy management and renewable integration, *Energ. Buildings* 323 (Nov. 2024) 114754, https://doi.org/10.1016/j.enbuild.2024.114754.

[18] M. Shang, Y. Zhu, Thermodynamic and exergoeconomic assessment of a trigeneration system driven by a biomass energy source for power, cooling, and heating generation, *Energy* 290 (Mar. 2024) 130085, https://doi.org/10.1016/j.energy.2023.130085.

[19] N. Zhang, P. Qin, Z. Zhao, H. Xu, T. Ouyang, Techno-economic evaluation and optimized design of new trigeneration system for residential buildings, *J. Clean. Prod.* 440 (Feb. 2024) 140917, https://doi.org/10.1016/j.jclepro.2024.140917.

[20] J. Jia, M.C. Paul, Thermodynamic and economic evaluation of a CCHP system with biomass gasifier, Stirling engine, internal combustion engine and absorption chiller, *Energ. Conver. Manage.* 299 (Jan. 2024) 117803, https://doi.org/10.1016/j.enconman.2023.117803.

[21] H.S.A. Turgut, I. Dincer, Development and assessment of a floating photovoltaic-based hydrogen production system integrated with storage options, *Process Saf. Environ. Prot.* 190 (Oct. 2024) 930–943, https://doi.org/10.1016/j.psep.2024.07.044.

[22] Z. Meng, K. Wang, J. Di, Z. Lang, Q. He, Energy analysis and exergy analysis study of a novel high-efficiency wind-hydrogen storage and power generation polygeneration system, *Int. J. Hydrogen Energy* 57 (Feb. 2024) 338–355, https://doi.org/10.1016/j.ijhydene.2024.01.013.

[23] A.J. White, Theoretical analysis of cavern-related exergy losses for compressed air energy storage systems, *J. Storage Mater.* 81 (Mar. 2024) 110419, https://doi.org/10.1016/j.est.2024.110419.

[24] M.C. Gilago, V.R. Mugi, V.P. Chandramohan, Investigation of exergy-energy and environ-economic performance parameters of active indirect solar dryer for pineapple drying without and with energy storage unit, *Sustainable Energy Technol. Assess.* 53 (Oct. 2022) 102701, https://doi.org/10.1016/j.seta.2022.102701.

[25] Y. Zhou, Z. Liu, A cross-scale 'material-component-system' framework for transition towards zero-carbon buildings and districts with low, medium and high-temperature phase change materials, *Sustain. Cities Soc.* 89 (Feb. 2023) 104378, https://doi.org/10.1016/j.scs.2022.104378.

[26] J.A. Bryan, H. Wang, P.W. Talbot, Sensitivity Analysis of a Nuclear Hybrid Energy System With Thermal Energy Storage in Deregulated Electricity Markets Considering Time Series Uncertainty in Electricity Price, *Energy Storage* 6 (8) (2024) e70082, https://doi.org/10.1002/est2.70082.

[27] C. Gao, Performance investigation of solar-assisted supercritical compressed carbon dioxide energy storage systems, *J. Storage Mater.* 79 (Feb. 2024) 110179, https://doi.org/10.1016/j.est.2023.110179.

[28] L.S. Budovich, Energy, exergy analysis in a hybrid power and hydrogen production system using biomass and organic Rankine cycle, *International Journal of Thermofluids* 21 (Feb. 2024) 100584, https://doi.org/10.1016/j.ijft.2024.100584.

[29] M. Sharifishourabi, I. Dincer, A. Mohany, Performance and environmental impact assessments of a newly developed multigeneration system for sustainable communities, *Process Saf. Environ. Prot.* 178 (Oct. 2023) 1119–1129, https://doi.org/10.1016/j.psep.2023.08.089.

[30] X. Chen, Z. Sun, P.-C. Kuo, M. Aziz, Carbon-negative olefins production from biomass and solar energy via direct chemical looping, *Energy* 289 (Feb. 2024) 129943, https://doi.org/10.1016/j.energy.2023.129943.

[31] Q. Hao, L. Zhu, Y. Wang, Y. He, X. Zeng, J. Zhu, Achieving near-zero emission and high-efficient combined cooling, heating and power based on biomass gasification coupled with SOFC hybrid system, *Fuel* 357 (Feb. 2024) 129751, https://doi.org/10.1016/j.fuel.2023.129751.

[32] M. Sharifishourabi, I. Dincer, A. Mohany, Performance and environmental impact evaluations of a novel multigeneration system with sonic hydrogen production and energy storage options, *J. Storage Mater.* 78 (Feb. 2024) 109987, https://doi.org/10.1016/j.est.2023.109987.

[33] G. Alarnaot-Alarnaout, J. Navarro-Esbrí, Á. Barragán-Cervera, A. Mota-Babiloni, Energy, exergy, economic, and environmental (4E) assessment of an experimental moderately-high-temperature heat pump for district heating and cooling networks, *Energ. Conver. Manage.* 325 (Feb. 2025) 119346, https://doi.org/10.1016/j.enconman.2024.119346.

[34] Y. Çengel, Ramifications of the 2nd law of thermodynamics on innovation and sustainable future, IJRIC 2 (2) (2019) 91, https://doi.org/10.1504/IJRIC.2019.104011.

[35] S.A. Opatokun, V. Strezov, T. Kan, Product based evaluation of pyrolysis of food waste and its digestate, Energy 92 (2015) 349–354, https://doi.org/10.1016/j.energy.2015.02.098.

[36] Z. Rahimimotlagh, A. Ahmadi, Energy, exergy, exergoeconomic and exergoenvironmental analysis and optimization of combined solar, SRC cycles with compressed air energy storage (CAES) and methane production system, *Energ. Conver. Manage.* 317 (Oct. 2024) 118855, https://doi.org/10.1016/j.enconman.2024.118855.

[37] P. Yin, F. Sardari, Process arrangement and multi-criteria study/optimization of a novel hybrid solar-geothermal scheme combined with a compressed air energy storage: Application of different MOPSO-based scenarios, *Energy* 282 (Nov. 2023) 128651, https://doi.org/10.1016/j.energy.2023.128651.